

# Geophysical Research Letters

## RESEARCH LETTER

10.1029/2018GL081334

### Key Points:

- Skilful dynamical seasonal prediction of ocean surface waves is improved
- We demonstrate NAO as a major source of seasonal predictability of waves in the Atlantic Ocean
- NAO-based subsampling improves seasonal prediction of ocean surface waves

### Supporting Information:

- Supporting Information S1

### Correspondence to:

M. Dobrynin,  
mikhail.dobrynin@uni-hamburg.de

### Citation:

Dobrynin, M., Kleine, T., Düsterhus, A., & Baehr, J. (2019). Skilful seasonal prediction of ocean surface waves in the Atlantic Ocean. *Geophysical Research Letters*, 46, 1731–1739. <https://doi.org/10.1029/2018GL081334>

Received 5 SEP 2018

Accepted 6 FEB 2019

Accepted article online 11 FEB 2019

Published online 14 FEB 2019

## Skilful Seasonal Prediction of Ocean Surface Waves in the Atlantic Ocean

Mikhail Dobrynin<sup>1</sup> , Tobias Kleine<sup>1</sup>, André Düsterhus<sup>1</sup> , and Johanna Baehr<sup>1</sup> 

<sup>1</sup>Institute of Oceanography, Center for Earth System Research and Sustainability (CEN), Universität Hamburg, Hamburg, Germany

**Abstract** Ocean surface wave height in the Atlantic Ocean is strongly influenced by the North Atlantic Oscillation (NAO). Here we demonstrate for the first time a skilful seasonal forecast for wave height in the Atlantic Ocean, produced by a seasonal prediction system with an enhanced prediction skill of winter NAO. The improved seasonal prediction skill of the wave height reaches 0.8 in major parts of the North Atlantic. Prediction skill in the Central and South Atlantic is significantly improved due to swell propagation from better represented active wave generation regions in the North Atlantic. By subsampling, the modeling of climatological anomalies of seasonal wave height for strongly positive and negative NAO phases is considerably improved. We demonstrate the potential of an improved, subsampling-based approach for the dynamical seasonal prediction of waves, specifically for extreme seasons during strong NAO phases, which can be implemented for operational purposes.

**Plain Language Summary** Ocean surface wave height in the Atlantic Ocean depends mainly on low-frequency atmospheric variability such as the North Atlantic Oscillation (NAO). Depending on the NAO phase, different weather regimes, mean, and extreme wind and wave conditions develop over the North Atlantic. The NAO affects the location and orientation of cyclone tracks and is therefore responsible for more frequent extreme storms during a strongly positive NAO phase. Here for the first time, we show that a state-of-the-art seasonal prediction system with an enhanced prediction of winter NAO leads to better forecasting of ocean waves in the Atlantic Ocean. In major parts of the North Atlantic, the classical ensemble mean approach demonstrated a prediction skill for the seasonal mean wave height of less than 0.5 for the hindcast period from 1982 to 2017. In contrast, the ensemble subsampling approach increased the skill to up to 0.8. Modeling of the seasonal mean wave height for strongly positive and negative NAO phases is considerably improved after subsampling. Thereby, we demonstrate the potential of a subsampling approach for the prediction of wave conditions during strong NAO phases.

### 1. Introduction

In the Atlantic Ocean, ocean surface waves show pronounced interannual variability (e.g., Semedo et al., 2018) along with a seasonal cycle. During storm seasons, typically from November to March, the monthly mean wave height can change from year to year by a factor of 2 (Woolf et al., 2002). The North Atlantic wind and surface ocean waves also experience a notable impact of ongoing climate change. Despite a projected decrease of wind speed and wave height in the North Atlantic (Hemer et al., 2013), an intensification of extreme events is expected in the near future (Dobrynin et al., 2012; Pinto et al., 2008; Weisse et al., 2005). In major parts of the North Atlantic changes in wind and wave climate will be already detectable in this decade (Dobrynin et al., 2014).

Storm dynamics in the North Atlantic has a typical time scale of days. However, a clear dependency between the storm's frequency and the low-frequency atmospheric variability such as the North Atlantic Oscillation (NAO) has been previously found (Gleeson et al., 2017; Rogers, 1997; Semedo et al., 2011; Wang & Swail, 2001). Depending on the NAO phase, different weather regimes (e.g., wind regimes; Cassou et al., 2011), mean, and extreme wind and wave conditions develop over the North Atlantic. Pinto et al. (2008) demonstrated that the NAO affects the location and orientation of the cyclone tracks and is therefore responsible for more frequent extreme storms during a strongly positive NAO phase. Donat et al. (2010) reported that only 5–7% of the storms in the North Atlantic occur during negative NAO phases. In contrast, many storms occur during a positive NAO phase. Strongly positive NAO phases are present for more than 20% of storms.

Previous attempts to predict the seasonal mean wave height were able to demonstrate low to moderate skill for various regions and periods. Bell and Kirtman (2018) analyzed the prediction of waves in the North Pacific focusing on ship routes during July. Lopez and Kirtman (2016) considered El Niño–Southern Oscillation as a potential source of wave height predictability in the West Pacific and Indian Oceans. Lopez and Kirtman (2016) indicated a potential for predicting wave heights in the Northwest Pacific and Bay of Bengal during boreal summer for several months ahead after a warm El Niño–Southern Oscillation phase. Colman et al. (2011) assessed the potential of a statistical categorized seasonal prediction of wave heights in the northern North Sea using a forecast of the NAO index.

In the Atlantic Ocean, further improvement of forecast skill can be expected from an improved ability of the prediction system to represent the sources of monthly and seasonal variability of wind and waves, which is strongly associated with the accuracy of seasonal prediction of winter NAO. Better representation of the region of active wave generation such as the northern North Atlantic may lead not only to a better prediction skill in regions of direct NAO impact but also, due to swell propagation, in remote regions such as the southern North Atlantic.

Some state-of-the-art ensemble-based seasonal prediction systems show a significant winter NAO prediction skill (e.g., Butler et al., 2016). For example, the 10-member seasonal prediction system based on the mixed resolution Coupled Model Intercomparison Project Phase 5 version of the Max Planck Institute for Meteorology Earth system model (MPI-ESM-MR; Giorgetta et al., 2013) shows a correlation (prediction skill) between observed and forecasted NAO index of 0.43. In the recent study by Dobrynin et al. (2018) this MPI-ESM-MR ensemble was extended to 30 members, where the prediction skill is improved to 0.52. Moreover, Dobrynin et al. (2018) suggested a teleconnection-based subsampling approach that increased the winter NAO prediction skill to up to 0.86.

In this study, we extend the ensemble presented by Dobrynin et al. (2018) to 2017 and use the 30-member ensemble provided by the Earth system model MPI-ESM-MR to force the spectral wave model WAM (The WAMDI Group, 1988) and generate an ocean wave seasonal prediction ensemble for the period from 1982 to 2017. Combined wave height (hereafter total wave height) of high-frequency locally generated wind wave (hereafter sea wave height), and low-frequency (hereafter swell wave height) parts of wave spectrum are separately analyzed. We concentrate on the winter NAO-related wave dynamics and possible improvements of prediction skill of wave height in both locally generated wind sea (hereafter wind sea) and the remotely generated swell parts of wave spectrum.

## 2. Setup and Methods

### 2.1. Design of a Dynamical Seasonal Prediction System for Ocean Surface Waves

For this study, MPI-ESM-MR is used as a basis for a dynamical seasonal prediction system (Baehr et al., 2015; Dobrynin et al., 2018) and extended by the spectral wave model WAM (The WAMDI Group, 1988). MPI-ESM-MR has a horizontal resolution of approximately  $1.8^\circ$  in the atmosphere and  $0.4^\circ$  in the ocean. The wave model WAM has a resolution of  $1^\circ$ . The spectral resolution of WAM covers 24 directional sectors with a step of  $7.5^\circ$  and has 25 frequency bands in a range from 0.042 to 0.41 Hz. According to the WAM separation scheme of the 2-D spectrum, a threshold frequency corresponding to wave phase speed is used for spectrum separation. Calculation of wind sea and swell parameters over high- and low-frequency parts of wave spectrum is separately conducted.

The prediction system consists of two major parts. The first part is an assimilation simulation for the ensemble initialization. The second part consists of a 30-member reforecast (hereafter MR-30) covering the period from 1982 to 2017. In the assimilation simulation, MPI-ESM-MR is initialized, using a full-field nudging technique, from the ERA-Interim reanalysis (Dee et al., 2011) in the atmosphere, from the ORA-S4 (Balmaseda et al., 2013) in the ocean, and from the NSIDC (Comiso, 1995) observations in the sea ice component. For the generation of initial perturbations, vertically varying bred vectors in the ocean were used (Baehr & Piontek, 2014). The MR-30 ensemble of reforecasts is initialized every November from the assimilation simulation. After initialization, the system runs freely for 6 months. Similar to the MPI-ESM-MR, the wave model WAM was first used to calculate an assimilation simulation using the 6-hourly wind speed and daily ice concentration from the MPI-ESM-MR assimilation simulation. The MR-30 ensemble was then extended by wave reforecasts (hereafter WAM-30) generated by WAM using wind and ice data from each member of MR-30 and initialized from WAM assimilation simulation every 1 November. The period of each

reforecast in WAM-30 is 6 months as in MR-30. The seasonal mean and extreme values of wave heights were calculated from the 6-hourly WAM-30 output.

## 2.2. NAO Index and Subsampling

We use an empirical orthogonal function (EOF) analysis (Barnston & Livezey, 1987) to calculate the boreal winter (averaged over December, January, and February; DJF) NAO index (Figure S1 in the supporting information). Seasonal (DJF) means of sea-level pressure (SLP) were used from the region limited to 20°N and 90°N latitudes and 90°W and 60°E longitudes. The EOF-based NAO index is represented by the principal component of the leading EOF of SLP (Kutzbach, 1970). In this study, we use the ERA-Interim NAO as a reference, and the ensemble-based seasonal prediction of NAO from Dobrynin et al. (2018), normalized by their respective standard deviations. We define years of strongly positive NAO<sup>+</sup> and negative NAO<sup>-</sup> phases as years with anomalies of the NAO that exceed the mean NAO value by  $\pm 1$  standard deviation. A mean NAO value over the entire period of the simulation is used as a reference for anomalies calculation.

Dobrynin et al. (2018) reported a subsampling method, which considers well-established NAO teleconnection such as links between the October sea surface temperature in the North Atlantic, snow depth in Eurasia, the stratospheric air temperature in the Northern Hemisphere, September sea ice volume in the Arctic, and the subsequent winter NAO. This allows to estimate a “first guess” of upcoming winter NAO already from the analysis of the autumn (initial) state of the Earth system. Combining the first guess NAO and dynamical seasonal ensemble, subsampling can be applied for the full ensemble. After subsampling only ensemble members are considered which show a NAO that is similar to first guess NAO index. In this study, we consider the winter NAO index and thereby the variability of the SLP as a potential source of predictability of seasonal mean significant wave height. Therefore, following Dobrynin et al. (2018), we apply subsampling to the dynamical ensemble of ocean waves WAM-30. Only ensemble members of WAM-30 forced by members of MPI-ESM-MR ensemble with a NAO similar to the first-guess NAO index are considered. Thereby, a new subsampled ensemble (WAM-Sub) is constructed.

## 2.3. Singular Value Decomposition Analysis of SLP and Wave Height

Previously, EOF analysis was used to analyze the modes of variability of wave height (e.g., Woolf et al., 2002). We apply a singular value decomposition (SVD) analysis to the assimilation simulation in order to demonstrate the ability of our seasonal prediction system to simulate the well-known dependencies between the SLP and wave height in the North Atlantic. In contrast to the EOF analysis, an SVD combines two different fields, here the wave height and SLP, and identifies only modes where the variability of both fields is strongly coupled.

## 2.4. Prediction Skill

The prediction skill is assessed in the hindcast period from 1982 to 2017 by the anomaly correlation coefficient (ACC; Collins, 2002). As a reference, we use the total significant wave height from the ERA-Interim wave reanalysis as an adequate alternative to wave observations as our focus is on seasonal time scales and open ocean areas. For the calculation of the ACC for the sea and swell significant wave heights, the assimilation simulation is used. ACCs for seasonal wave heights both from the WAM-30 ensemble mean and the subsampled ensemble mean are calculated.

For a selected region of strong NAO impact in the northeastern part of the North Atlantic, prediction skill for area averaged time series of wave height is analyzed in terms of ACC and root-mean-square error (RMSE). The significance of correlation at the 95th confidence level is calculated using a bootstrapping test with 500 samples.

## 3. Common Modes of SLP Waves Variability

An SVD is calculated for the seasonal means of the total, wind sea, and swell significant wave heights and SLP (Figure 1). For the coupled SLP wave height covariations, the leading SVD mode explains 64%, 61%, and 65% of covariance for total, sea, and swell significant wave height, respectively. As a measure of coupling of the SLP variability and the wave height, we calculate the correlations between the SLP and the expansion coefficient of the total, wind sea, and swell significant wave height in the assimilation simulation from 1982 to 2017. The horizontal distribution of correlation patterns indicates that in major parts of the North Atlantic the seasonal variability of wave height is dominated by SLP variability (Figure 1). However, for high- and

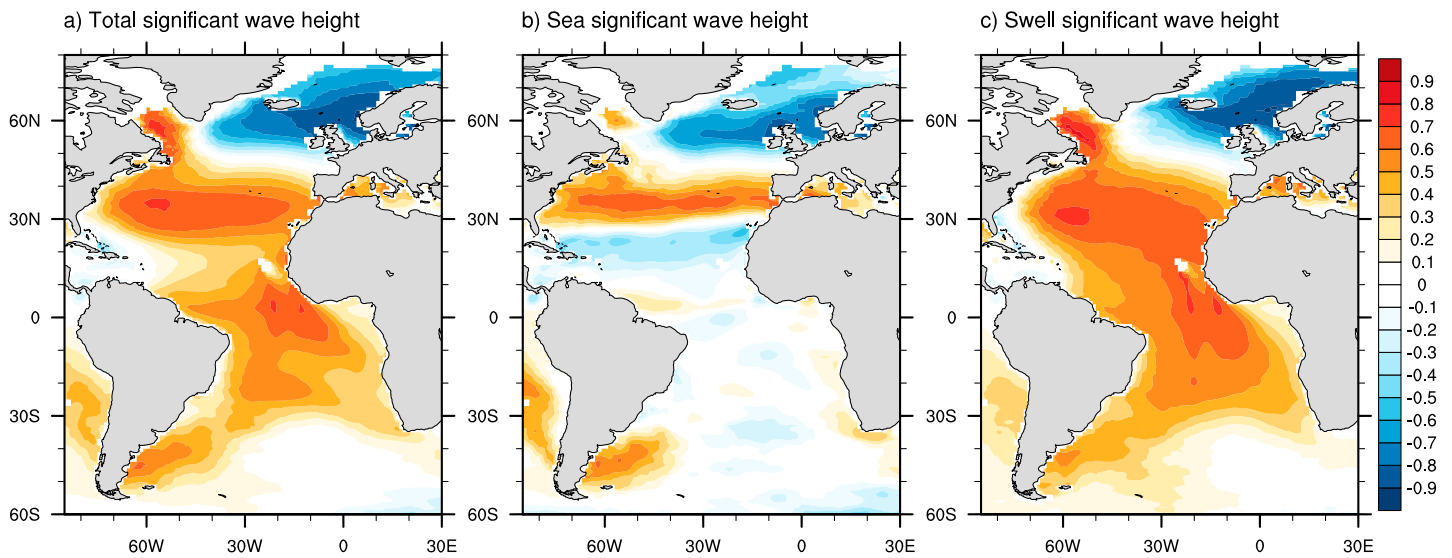


**Figure 1.** Singular value decomposition of sea-level pressure and significant wave heights. Correlation between sea-level pressure and the expansion coefficient of the total (a), sea (b), and swell (c) significant wave height calculated in the assimilation simulation from 1982 to 2017.

low-frequency parts of the wave spectrum, represented by sea and swell significant wave height, the patterns of correlation are different in relation to each other in the equatorial and South Atlantic.

For wind sea waves generated by local wind, the high correlation regions are clearly associated with SLP variability, with a zone of low SLP variability in the leading mode separating the positive and negative centers of SLP variability (Figure 1b). The zones of positive and negative correlations toward South and North from the “zero” line indicate zones of locally generated waves. The positive correlation pattern can be associated with westerlies (prevailing winds in the middle latitudes range from about 30°N to 60°N). The negative anomaly north of the subpolar low-pressure zone is related to polar easterlies, the dominant wind system in the polar region. Both regions can be indicated as southern (hereafter SSG) and northern (hereafter NSG) swell generation regions, wherefrom locally generated wind waves propagate toward the South Atlantic and into the Arctic.

For swell (Figure 1c), a large area of the Atlantic shows a high positive correlation which is related to NAO-dependent origin of swell in wave generation regions in the North Atlantic. Due to geographical locations, the SSG region dominates the subtropical, equatorial, and southern parts of the Atlantic. To some extent swell generated in the SSG region also impacts the NSG region. Stronger pronounced negative correlations in the polar region comparing wind sea and swell are most likely also related to propagation of swell from the SSG region. The high positive correlations in the Labrador Sea can be attributed to the NSG region. In the South Atlantic, the impact of NAO variability and swell propagation from the North Atlantic is lower, because of the stronger effect of swell generated in the Southern Ocean.

In summary, a short qualitative analysis of correlation patterns indicates two zones of a strong effect of SLP variability on the generation of waves: the midlatitudes and the eastern part of subpolar North Atlantic.

## 4. Effect of Subsampling on Seasonal Prediction Skill of Wave Height

### 4.1. Improvement of Seasonal Prediction Skill

We apply the subsampling approach of Dobrynin et al. (2018) to WAM-30 for the period from 1982 to 2017. The prediction skill of the seasonal (DJF) mean for total, wind sea, and swell significant wave heights is assessed by ACCs calculated between the assimilation simulation, the full WAM-30 ensemble, and for the subsampled WAM-Sub ensemble (Figure 2). Although the SVD analysis indicates major parts of the Atlantic as a zone of common variability of SLP and waves, the prediction skill patterns for WAM-30 ensemble mean have a different, more fragmented structure (Figure 2, left column). WAM-30 shows low to moderate prediction skill of up to 0.6 in the subpolar and middle latitudes (both in the North and South Atlantic) regions. This can be attributed to dominant wind systems with high persistence in these regions. Comparing the prediction skill for total, sea, and swell significant wave height, we note that the sea wave height has higher

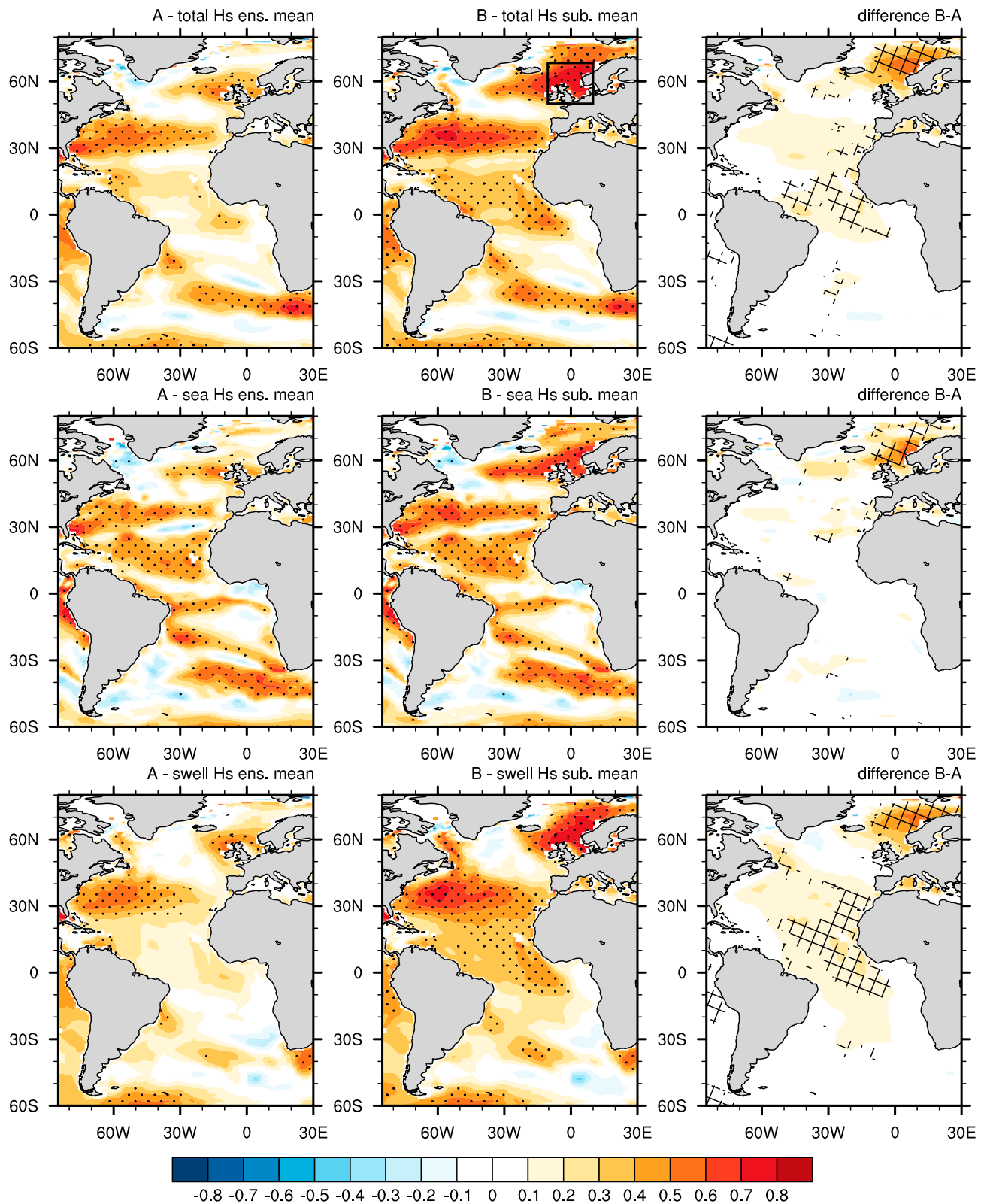


**Figure 2.** Improvement of the prediction of significant wave height in the Atlantic ocean due to more accurate prediction of the winter North Atlantic Oscillation. Anomaly correlation coefficient calculated for WAM-30 (left column) and WAM-Sub (middle column) and their difference (right column) relative to the assimilation simulation for total wave height (top row), sea height (middle row), and swell height (bottom row). Regions that are significant at the 95% confidence level are indicated by dots on the maps in the left and middle columns. Hashing in the right column indicates regions that became significant after subsampling. The region for the time series analysis is indicated (black frame).

than swell wave height skill in the tropical and equatorial parts of the Atlantic. However, this signal is not represented in the total wave height, decreased by very low prediction skill for swell in these regions. After subsampling, the prediction skill for swell is strongly improved (Figure 2, middle and right columns) in the areas of NAO impact, such as in the subpolar, tropical, and equatorial parts of the Atlantic. The result is now more consistent with SVD analysis than WAM-30. The area, where prediction skill for the sea wave height becomes significant, is smaller than the area for swell. For total wave height, the prediction skill improved by both sea and swell parts of the wave spectrum. After subsampling two major regions in the eastern polar sector and equatorial parts of Atlantic become significant (Figure 2, right column).

#### 4.2. Improvement of Anomalies for Strong NAO Phases

The potential of a seasonal wave prediction system to represent wave dynamics in the North Atlantic according to changes in NAO phases can be assessed by calculating climatological winter (DJF) composite anomalies of wave height for positive and negative phases of the winter NAO (NAO<sup>±</sup>). For strong NAO<sup>+</sup> phases and strong NAO<sup>-</sup> phases a clear dipole pattern of wave height anomalies is shown in the assimilation simulation from 1982 to 2017 using a mean over this period as a reference for the anomalies (Figures S2a and S2b). For NAO<sup>+</sup>, a positive anomaly is located in the subpolar region, whereas a negative anomaly appears in the midlatitudes of the North Atlantic. For NAO<sup>-</sup>, the sign of the wave anomalies changes, but the geographical location of anomalies remains similar for both negative and positive NAO phases.

For both phases, the location of wave height anomalies is consistent with the location of zones of strongest covariability of SLP and wave height. Comparing winter anomalies of wave height calculated from the WAM-30 ensemble mean (Figures S2c and S2d) with anomalies from the assimilation simulation (Figures S2a and S2b), we conclude that the WAM-30 ensemble mean cannot reproduce the dipole structure of wave height anomalies. Despite the relatively high prediction skill of the winter NAO in MR-30, the change of wave dynamics in the North Atlantic depending on the winter NAO phase is only resolved to a small extent.

In contrast, considering only ensemble members with accurate representation of the NAO through subsampling (winter NAO prediction skill is 0.85), the WAM-Sub tends to represent the wave height anomalies much more pronounced (Figures S2e and S2f) as compared to WAM-30 (Figures S2c and S2d). However, the amplitude of anomalies of wave height for both NAO<sup>+</sup> and NAO<sup>-</sup> phases is still lower, compared to assimilation simulation.

#### 4.3. Potential Impact of Subsampling in the Northeastern Atlantic

As previously reported by Woolf et al. (2002), a region in the northeastern Atlantic has high potential to improve the prediction skill for waves due to a better representation of the winter NAO. Indeed, combining our previous analysis of SVD, ACC, and anomalies, we can estimate an area of maximum impact of the winter NAO on waves in a region limited to a range of latitude from 50°N to 68°N and to a range of longitude from 10°W to 10°E. This region shows covariability of SLP and waves (Figure 1a), strong improvement in ACC (Figure 2), and the highest anomalies of seasonal wave heights associated with strong NAO<sup>+</sup> phase. For that region, we now calculate an area weighted mean and extremes (99th percentile over a winter season) of the total, wind sea, and swell significant wave height for WAM-30 ensemble mean and for WAM-Sub ensemble mean (Figure 3). These time series are analyzed in terms of the correlation between the wave heights from the ERA-Interim and from the assimilation simulation and both from the WAM-30 ensemble mean and WAM-Sub ensemble mean. The values of correlations are summarized in tables embedded in each subplot of Figure 3.

The maximum of the possible impact of the winter NAO on the wave height dynamics (hereafter NAO impact) can be estimated as a value of correlation between the time series of ERA-Interim winter NAO index and wave height calculated in the assimilation simulation. This correlation varies from 0.92 for mean wave height to 0.83 for extremes. However, considering the moderate level of NAO prediction in the hindcast, the relationship between NAO and predicted wave height might be weaker. In the hindcast, the correlation between the ensemble mean wave height and the NAO index varies between 0.46 and 0.49 for mean wave height and for the extremes, respectively (Figures 3a and 3b). This indicates a weaker response of the wave dynamics to the winter NAO in the hindcast compared to assimilation run (see Figure 3 and Table S1).

Over the hindcast period from 1982 to 2017, we find a low to moderate prediction skill for WAM-30 ensemble mean for total significant wave height. The prediction skill is in a range from 0.32 for mean (Figure 3a) to 0.27 for extremes values (Figure 3b), when compared to ERA-Interim. Comparing to the assimilation

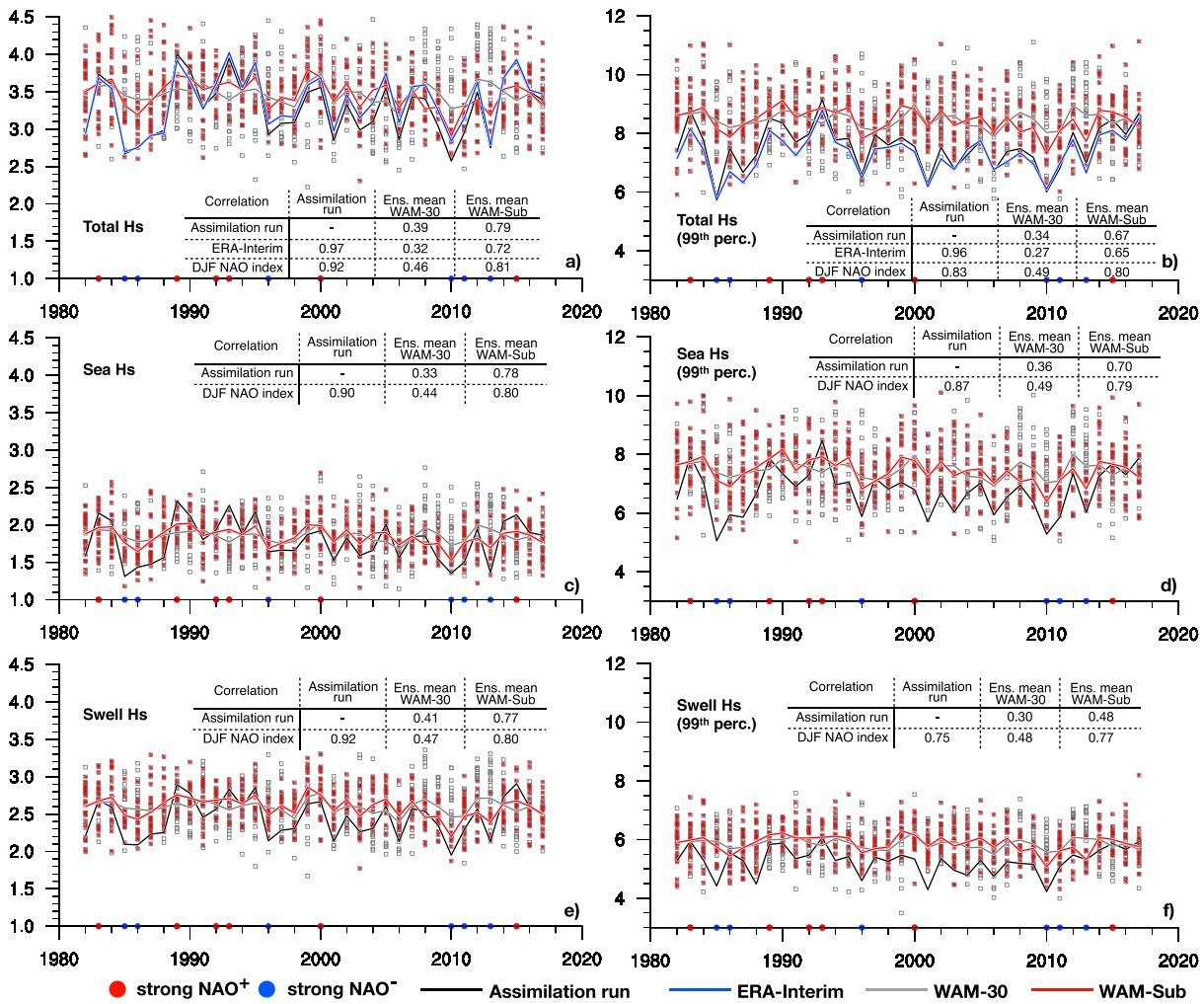


**Figure 3.** Time series of DJF mean and 99th percentile of significant wave heights (m) in the North Atlantic. December, January, and February (DJF) mean (left column) and DJF 99th percentile (right column) of total (a, b), sea (c, d), and swell (e, f) significant wave heights. Gray squares represent each individual ensemble member (gray line represents ensemble mean), red-filled squares indicate selected members with the accurate representation of the winter NAO according to Dobrynin et al. (2018; red line indicates the subsampled ensemble mean), black line represents assimilation simulation, and blue line represents ERA-Interim. Time series of wave heights are calculated as an area mean in the region of strong NAO impact on waves from Figure 2 and limited according to the latitude range 50°N–68°N and the longitude range 10°W–10°E. Values of correlation between the time series are summarized in tables. Correlations are significant at the 95th confidence level, according to a bootstrapping test with 500 samples. NAO = North Atlantic Oscillation.

simulation, a slightly higher prediction skill was found, from 0.34 for extremes to 0.39 for mean wave height. In terms of RMSE (Table S1) for total significant wave height, the range varies from 1.32 m for extreme to 0.36 m for mean values, compared to the ERA-Interim, and from 1.32 to 0.36 m, compared to the assimilation simulation.

Since the wind sea and swell wave heights are not available from the ERA-Interim, we compare these two parts of the wave spectrum to the assimilation simulation only. For wind sea and swell wave height we find a similar level of prediction skill (hereafter the RMSE is shown in parentheses) of 0.33 (0.26 m) for mean wind sea height, 0.41 (0.27 m) for mean swell height, and 0.36 (1.01 m) and 0.30 (0.73 m) for the extremes of wind sea and swell heights (Figures 3c–3f). In summary, the WAM-30 ensemble demonstrates a moderate level of predictability of seasonal mean (DJF) of total, wind sea, and swell significant wave height. Comparing the correlation between the NAO index and the wave height time series from the assimilation simulation and from the WAM-30 ensemble mean, we conclude that our system shows potential to improvement of prediction skill due to subsampling.

Finally, the WAM-Sub ensemble demonstrates a significant improvement of prediction skill for total wave height from 0.32 to 0.72 for mean wave height and from 0.27 to 0.65 for extreme values (Figures 3a and 3b). The NAO impact is increased after subsampling to 0.81 for mean and to 0.80 for extreme wave height, compared to 0.46 and 0.49 before subsampling (Figures 3a and 3b). The full WAM-30 ensemble mean generally tends to overestimate the mean wave height during strongly negative NAO phases and underestimate the wave height for the years with strongly positive NAO phases (Figures 3a, 3c, and 3e). This is improved with the application of subsampling. For extreme values of wave heights, the full WAM-30 ensemble overestimates the wave height for both, strongly positive and strongly negative NAO phases (Figures 3b, 3d, and 3f). The RMSE decreases due to subsampling both for extremes and for mean values, compared to either ERA-Interim or the assimilation simulation (Table S1). Comparing the improvement in prediction skill for extreme wind sea and swell wave height, it appears that following lower NAO impact on swell in this region (0.75, Figures 3d and 3f), the improvement for swell height is small (from 0.30 to 0.48, before and after subsampling), whereas for wind sea wave height with higher NAO impact (0.87, Figure 3d) the improvement is more pronounced (from 0.36 to 0.70, before and after subsampling).

The NAO signal for weak NAO phases (all years of the time series excluding those with strong NAO phases) is less pronounced. Therefore, in line with the subsampling method, the effect of subsampling is expected to be much smaller for weak NAO phases compared to strong NAO phases. Indeed, from the analysis of years of weak NAO phases only, we conclude that for the total wave height the prediction skill improves due to subsampling from 0.50 to 0.62 and from 0.30 to 0.41 for seasonal mean and extreme values, respectively. Weak NAO phases have no pronounced effect on swell prediction. Therefore, the prediction skill of swell is not changed significantly due to subsampling from 0.54 to 0.58 and from 0.28 to 0.25 for seasonal mean and extreme values respectively. The impact of weak NAO phases on wind sea wave height is more notable comparing to swell. We calculate the improvement of prediction skill for wind sea wave height from 0.42 to 0.65 and from 0.31 to 0.39 for seasonal mean and extreme values, respectively (see Table S2 for more details).

## 5. Summary and Conclusions

Improved seasonal prediction of wave height is analyzed for the Atlantic Ocean. The impacts of well-predicted winter NAO on the accuracy of total wave height forecasts, as well as high-frequency (wind sea), and low-frequency (swell) parts of the wave spectrum, were separately analyzed. We conclude that following an extended dependency of the ocean surface waves seasonal dynamics on the NAO state, in major parts of the Atlantic Ocean, the wave height can be accurately predicted for the upcoming winter season. From the analysis of the NAO teleconnections based subsampling approach applied to a dynamical 30-member ensemble of wave hindcasts, we conclude the following: The improvement in the prediction of the seasonal mean wave height is mostly found in the eastern parts of the subpolar and polar sectors and tropical and equatorial parts of the Atlantic in the Northern Hemisphere. Better representation of active wave generation regions in the North Atlantic leads to improved results in the Central and South Atlantic due to swell or low-frequency parts of the wave spectrum. In the tropical and equatorial regions of the North Atlantic and, to a small extent, of the South Atlantic, a significant improvement in the prediction of swell was found. The representation of seasonal mean wave height for strongly positive and negative NAO phases was considerably improved after subsampling. In the regions of strong NAO impact on the seasonal dynamics of waves in the northeastern part of the North Atlantic, the prediction for the area-averaged time series of mean and extreme wave height is enhanced. We demonstrate that the analysis of autumnal initial conditions of the NAO teleconnections improves the prediction of the seasonal mean wave height. This is particularly important for the prediction of extreme winter seasons in the North Atlantic during strongly positive phases of the winter NAO. From these results, the potential for improvement of operational seasonal wave forecast was demonstrated.

## References

- Baehr, J., Fröhlich, K., Botzet, M., Domeisen, D., Kornblueh, L., Notz, D., et al. (2015). The prediction of surface temperature in the new seasonal prediction system based on the MPI-ESM coupled climate model. *Climate Dynamics*, *44*(9-10), 2723–2735.
- Baehr, J., & Piontek, R. (2014). Ensemble initialization of the oceanic component of a coupled model through bred vectors at seasonal-to-interannual timescales. *Geoscientific Model Development*, *7*(1), 453–461.
- Balmaseda, M. A., Mogenssen, K., & Weaver, A. T. (2013). Evaluation of the ECMWF ocean reanalysis system ORAS4. *Quarterly Journal of the Royal Meteorological Society*, *139*(674), 1132–1161.

### Acknowledgments

This work was funded by the Deutsche Forschungsgemeinschaft (DFG, German Research Foundation) under Germany's Excellence Strategy - EXC 2037 'Climate, Climatic Change, and Society' - Project Number: 390683824, contribution to the Center for Earth System Research and Sustainability (CEN) of Universität Hamburg. Model simulations were performed using the high-performance computer at the German Climate Computing Center (DKRZ). Model data are accessible at the DKRZ ([www.dkrz.de/up](http://www.dkrz.de/up)). The authors would like to thank James Imber for valuable comments and proofreading of the manuscript.

- Barnston, A. G., & Livezey, R. E. (1987). Classification, seasonality and persistence of low-frequency atmospheric circulation patterns. *Monthly Weather Review*, *115*(6), 1083–1126.
- Bell, R., & Kirtman, B. (2018). Seasonal forecasting of winds, waves and currents in the North Pacific. *Journal of Operational Oceanography*, *11*(1), 11–26.
- Butler, A. H., Arribas, A., Athanassiadou, M., Baehr, J., Calvo, N., Charlton-Perez, A., et al. (2016). The climate-system historical forecast project: Do stratosphere-resolving models make better seasonal climate predictions in boreal winter? *Quarterly Journal of the Royal Meteorological Society*, *142*(696), 1413–1427.
- Cassou, C., Minvielle, M., Terray, L., & PÉrigaud, C. (2011). A statistical dynamical scheme for reconstructing ocean forcing in the Atlantic. Part I: Weather regimes as predictors for ocean surface variables. *Climate Dynamics*, *36*(1-2), 19–39.
- Collins, M. (2002). Climate predictability on interannual to decadal time scales: The initial value problem. *Climate Dynamics*, *19*(8), 671–692.
- Colman, A. W., Palin, E. J., Sanderson, M. G., Harrison, R. T., & Leggett, I. M. (2011). The potential for seasonal forecasting of winter wave heights in the northern North Sea. *Weather and Forecasting*, *26*(6), 1067–1074.
- Comiso, J. C. (1995). SSM/I sea ice concentrations using the bootstrap algorithm (Vol. 1380). National Aeronautics and Space Administration, Goddard Space Flight Center.
- Dee, D., Uppala, S., Simmons, A., Berrisford, P., Poli, P., Kobayashi, S, et al. (2011). The ERA-Interim reanalysis: Configuration and performance of the data assimilation system. *Quarterly Journal of the Royal Meteorological Society*, *137*(656), 553–597.
- Dobrynin, M., Domeisen, D. I., Müller, W. A., Bell, L., Brune, S., Bunzel, F., et al. (2018). Improved teleconnection-based dynamical seasonal predictions of boreal winter. *Geophysical Research Letters*, *45*, 3605–3614. <https://doi.org/10.1002/2018GL077209>
- Dobrynin, M., Murawski, J., Baehr, J., & Ilyina, T. (2014). Detection and attribution of climate change signal in ocean wind waves. *Journal of Climate*, *28*(4), 1578–1591.
- Dobrynin, M., Murawski, J., & Yang, S (2012). Evolution of the global wind wave climate in CMIP5 experiments. *Geophysical Research Letters*, *39*, L18606. <https://doi.org/10.1029/2012GL052843>
- Donat, M. G., Leckebusch, G. C., Pinto, J. G., & Ulbrich, U. (2010). Examination of wind storms over Central Europe with respect to circulation weather types and NAO phases. *International Journal of Climatology*, *30*(9), 1289–1300.
- Giorgetta, M. A., Jungclaus, J., Reick, C. H., Legutke, S., Bader, J., Böttinger, M., et al. (2013). Climate and carbon cycle changes from 1850 to 2100 in MPI-ESM simulations for the coupled model intercomparison project phase 5. *Journal of Advances in Modeling Earth Systems*, *5*, 572–597. <https://doi.org/10.1002/jame.20038>
- Gleeson, E., Gallagher, S., Clancy, C., & Dias, F. (2017). NAO and extreme ocean states in the Northeast Atlantic Ocean. *Advances in Science and Research*, *14*, 23.
- Hemer, M. A., Fan, Y., Mori, N., Semedo, A., & Wang, X. L. (2013). Projected changes in wave climate from a multi-model ensemble. *Nature Climate Change*, *3*(5), 471–476.
- Kutzbach, J. E. (1970). Large-scale features of monthly mean Northern Hemisphere anomaly maps of sea-level pressure. *Monthly Weather Review*, *98*(9), 708–716.
- Lopez, H., & Kirtman, B. P. (2016). Investigating the seasonal predictability of significant wave height in the West Pacific and Indian Oceans. *Geophysical Research Letters*, *43*, 3451–3458. <https://doi.org/10.1002/2016GL068653>
- Pinto, J. G., Zacharias, S., Fink, A. H., Leckebusch, G. C., & Ulbrich, U. (2008). Factors contributing to the development of extreme North Atlantic cyclones and their relationship with the NAO. *Climate Dynamics*, *32*(5), 711–737. <https://doi.org/10.1007/s00382-008-0396-4>
- Rogers, J. C. (1997). North Atlantic storm track variability and its association to the North Atlantic Oscillation and climate variability of northern Europe. *Journal of Climate*, *10*(7), 1635–1647.
- Semedo, A., Dobrynin, M., Lemos, G., Behrens, A., Staneva, J., de Vries, H., et al. (2018). CMIP5-derived single-forcing, single-model, and single-scenario wind-wave climate ensemble: Configuration and performance evaluation. *Journal of Marine Science and Engineering*, *6*(3), 90. <https://doi.org/10.3390/jmse6030090>
- Semedo, A., Sušelj, K., Rutgersson, A., & Sterl, A. (2011). A global view on the wind sea and swell climate and variability from ERA-40. *Journal of Climate*, *24*(5), 1461–1479.
- The WAMDI Group (1988). The WAM model—A third generation ocean wave prediction model. *Journal of Physical Oceanography*, *18*(12), 1775–1810.
- Wang, X., & Swail, V. (2001). Changes of extreme wave heights in Northern Hemisphere oceans and related atmospheric circulation regimes. *Journal of Climate*, *14*, 2204–2221.
- Weisse, R., von Storch, H., & Feser, F. (2005). Northeast Atlantic and North Sea storminess as simulated by a regional climate model 1958-2001 and comparison with observations. *Journal Climate*, *18*(3), 465–479.
- Woolf, D. K., Challenor, P., & Cotton, P. (2002). Variability and predictability of the North Atlantic wave climate. *Journal of Geophysical Research*, *107*(C10), 14.